Comparative Medicine
Copyright 2012
by the American Association for Laboratory Animal Science

Vol 62, No 5
August 2012
Pages 264–270

Original Research

Aortic Response to Balloon Injury in Obese Zucker Rats

Ludwig D Orozco,[1,*] Huiling Liu,[1] Betty B Chen,[1] Razvan F Buciuc,[1,2] Jonathan D Fratkin,[3] Juan C Pisarello,[1] and Eddie Perkins[1,4]

The small diameter of the carotid artery is not compatible with the evaluation of clinically available endovascular devices in the carotid balloon-injury (BI) model. We developed an endovascular BI model in the rat descending aorta, whose size is compatible with available endovascular instruments. We also tested the hypothesis that neointima formation is enhanced in the aorta of obese Zucker rats (OZR) compared with lean Zucker rats (LZR). Left external carotid arteriotomies and BI of the thoracic and abdominal aorta were performed by using a balloon catheter. Aortograms and aortic pathology were examined at 2, 4, and 10 wk after BI. At 10 wk after BI, the abdominal aorta in OZR had narrowed 8.3% ± 1.1% relative to baseline compared with an expansion of 2.4% ± 2.2% in LZR. Simultaneously, the thoracic aorta had expanded 9.5% ± 4.3% in LZR compared with stenosis of 2.8% ± 1.6% in OZR. Calculation of the intimal:medial thickness ratio revealed significantly increased neointimal formation in the OZR descending aorta compared with that in LNR. In conclusion, this minimally invasive BI model involving the rat descending aorta is compatible with available endovascular instruments. The descending aorta of OZR demonstrates enhanced neointimal formation and constrictive vascular remodeling after BI.

Abbreviations: BI, balloon injury; LZR, lean Zucker rats; OZR, obese Zucker rats.

Many endovascular interventions, either cardiovascular or neurovascular, involve balloon-angioplasty or stenting of stenosed or vasospastic arteries. Balloon injury (BI) to the arterial wall is well known to induce restenosis, with a typical decrease in lumen diameter as a result of intimal hyperplasia and vessel wall remodeling.[4,5,6,15,17,18] Restenosis occurs more frequently in patients with additional cardiovascular risk factors including diabetes, dyslipidemia, obesity, and hypertension.[4,8,23] Zucker rats frequently are used as animal models of obesity, dyslipidemia, and type 2 diabetes.[16,20,24]

The rat common carotid artery BI model is widely applied to study molecular mechanisms and the role of smooth muscle cells in arterial disease and healing.[17] Data on injury in other arteries and models are not extensive.[5] From a clinical perspective, the rat carotid artery is too small to test available endovascular devices. Other sites that have been used in rat models include the infrarenal aorta and the common iliac artery.[4,5,11,13,15,25] The aortic model requires an open laparotomy, whereas the common iliac artery is another small-caliber vessel. The goal of the present study was to create a minimally invasive BI model in the rat descending aorta that would be compatible with many endovascular instruments and implantable devices, such as stents, that are used currently in clinical practice.[15]

Materials and Methods

Lean (LZR; $n = 21$) and obese (OZR; $n = 21$) male Zucker diabetic rats (age, 10 wk) were obtained from Genetic Models (Indianapolis, IN). When the rats were 12 wk old, endovascular BI of the aorta was induced in the suprarenal abdominal and thoracic aorta. Rats were allocated randomly into 3 groups for study at 2 wk (6 LZR and 6 OZR), 4 wk (6 LZR and 6 OZR), and 10 wk (9 LZR and 9 OZR) after BI.

The rats had free access to rat chow (Harlan laboratories, Indianapolis, IN) and tap water acidified to pH 4.0. They were maintained at constant humidity (60% ± 5%), temperature (24 ± 1 °C), and light cycle (lights on, 0600 to 1800). All protocols were approved by the IACUC at the University of Mississippi Medical Center and were consistent with the *Guide for the Care and Use of Laboratory Animals*.[9]

Surgical technique. Inhalational anesthesia was induced with isoflurane as previously described.[12] The balloon catheter was introduced into the left carotid artery because it provides direct access into the descending aorta, thereby circumventing the difficulty of navigating the rather rigid balloon catheter system through the aortic arch (Figure 1). A left paramedian neck incision was performed, and the skin and sternocleidomastoid, omohyoid, and thyrohyoid muscles were retracted by using 3-0 polyglactin 910 sutures. Under microscopic magnification, the left common, internal, and external carotid arteries were exposed. The external carotid artery was ligated 6 mm distal to the carotid bifurcation by using 5-0 silk suture. The proximal common and internal carotid arteries (including the occipital artery) were clamped temporarily by using loops of 5-0 silk suture. The superior thyroid artery was coagulated by using bipolar cautery where it branched off the proximal external carotid artery. Lidocaine (5 mg/kg) was applied to prevent vasospasm.

Endovascular technique. A deflated balloon catheter (diameter, 3.25 mm; length, 9 mm; Gateway PTA, Boston Scientific, Natick,

Received: 23 Jan 2012. Revision requested: 08 Mar 2012. Accepted: 10 Mar 2012.
Departments of [1]Neurosurgery, [2]Radiology, [3]Pathology, and [4]Anatomy, University of Mississippi Medical Center, Jackson, Mississippi.
[*]Corresponding author. Email: lorozco-castillo@umc.edu

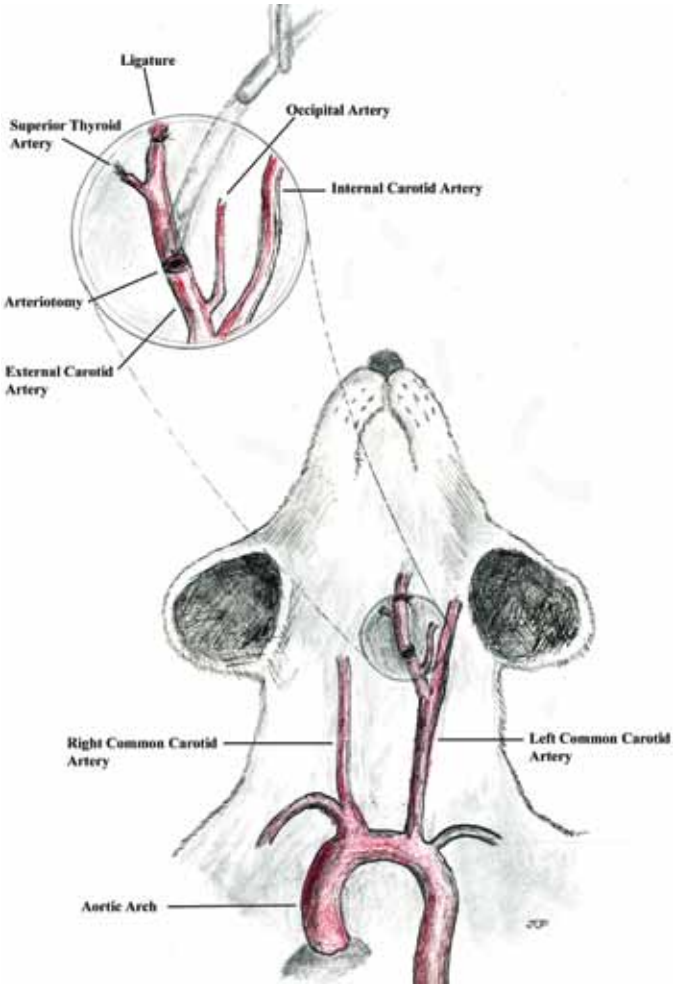

Figure 1. Illustration of the cervical arteries used to access the descending aorta. Left external carotid arteriotomy was used to introduce the balloon-catheter system, avoiding the acutely angled junction between the right common carotid artery and aortic arch junction. For follow-up aortograms, the flexible microcatheter wire was introduced through either right or left common carotid arteriotomy. Reproduced with permission.

MA) was inserted, through a transverse arteriotomy, into the proximal left external carotid artery and advanced to the common carotid artery. The temporary clamp on the common carotid artery was loosened, and a microwire (Agility-10, Cordis, Miami, FL) was navigated, inside the balloon catheter, to the descending aorta. Next, the balloon catheter was advanced, over the wire, to the proximal descending aorta. Baseline thoracic and abdominal aortograms were obtained by using the balloon catheter (without the microwire) and injecting 0.6 to 0.8 mL undiluted iohexol (Omnipaque-300, General Electric Healthcare, Princeton, NJ).

The abdominal aorta was injured by advancing the microwire to the infrarenal abdominal aorta, followed by the deflated balloon (over the wire), to just above the renal artery bifurcation. At this position, the balloon was inflated to a pressure of 2 atm (manual barometer) by using 50% diluted iohexol and pulled and rotated, from distal to proximal, over a 15-mm segment, 4 times (Figure 2). The balloon pressure was maintained at a constant pressure of 2 atm during the pulling phase. If significant resistance was encountered, the pressure was briefly lowered to 1.8 atm and then increased back to 2 atm. The pulling phase occurred immediately after balloon inflation and lasted for less than 15 to 20 s at a time. The thoracic aortic was injured in similar fashion from just above the diaphragm to a few millimeters distal to the aortic arch, over a 15-mm segment (Figure 2). This process denudes the vessel of endothelium and disrupts the elastic lamina and underlying smooth muscle cells.

Aortograms were obtained after BI to evaluate the injured areas for any immediate complications (dissection, rupture, thrombosis, occlusion; Figure 2). The balloon catheter was then removed, and the external carotid artery ligated proximal to the arteriotomy by using 5-0 silk. The temporary loops were removed from the common and internal carotid arteries, to restore perfusion. The neck was closed in a single layer of continuous 2-0 polyglactin 910 suture.

Microangiography of injured aortic arteries. At the appropriate follow-up time, either left or right paramedian neck incision was performed, and the common carotid artery was exposed and ligated proximal to the bifurcation by using a 5-0 silk suture. A proximal common carotid artery suture loop was applied, and a transverse arteriotomy was performed to allow access of a microcatheter (Prowler Plus, Cordis) with a microwire (Agility-10, Cordis). This microcatheter–wire system is more flexible and easier to navigate than is the balloon catheter, allowing its use in the angled, right carotid approach (Figure 1). The microcatheter was advanced over the wire to the proximal descending aorta, and thoracoabdominal aortograms were obtained (Figure 3). The microcatheter and wire were removed and the rat euthanized.

A picture archiving and communication system (iSite, Koninklijke Philips, Eindhoven, Netherlands) was used to analyze the pre- and postinjury aortograms. We considered 2 important factors when comparing measurements of the angiographic diameter of the aorta. First, the diameter of descending aorta varies along its length, with a wider proximal thoracic aorta that tapers down around the diaphragm and then widens again at the renal artery bifurcation (Figure 3). Second, the aortic size increases in diameter as the rats age and gain weight.[21] To correct for this variable aortic diameter, we calculated the baseline taper percentage and the postinjury stenosis or expansion percentages by adapting and applying the NASCET[3] formula.

Histomorphometry of injured aortic arteries. The entire aorta was harvested, and the adipose and adventitial layers were surgically removed. These vessels were placed in 2% (g/mL) paraformaldehyde (Sigma-Aldrich, St Louis, MO) in PBS for 24 h, followed by ethanol dehydration and paraffin embedding. Thin (10 µm) cross-sections were obtained at 1-mm intervals from injured and uninjured (control) segments. The sections were mounted on microscopic slides and stained with hematoxylin and eosin and trichrome stain.

A computer imaging system equipped with Metamorph version 6.37 (Molecular Devices, Sunnyvale, CA) was used to perform histomorphometric analysis of sectioned vessels. Medial and intimal thicknesses were measured at the point of maximal intimal hyperplasia. The media was limited by the internal and external elastic laminae. The intima was measured between the internal elastic lamina and the vessel lumen. The intimal:medial thickness ratio was calculated and used as an index of vascular injury.

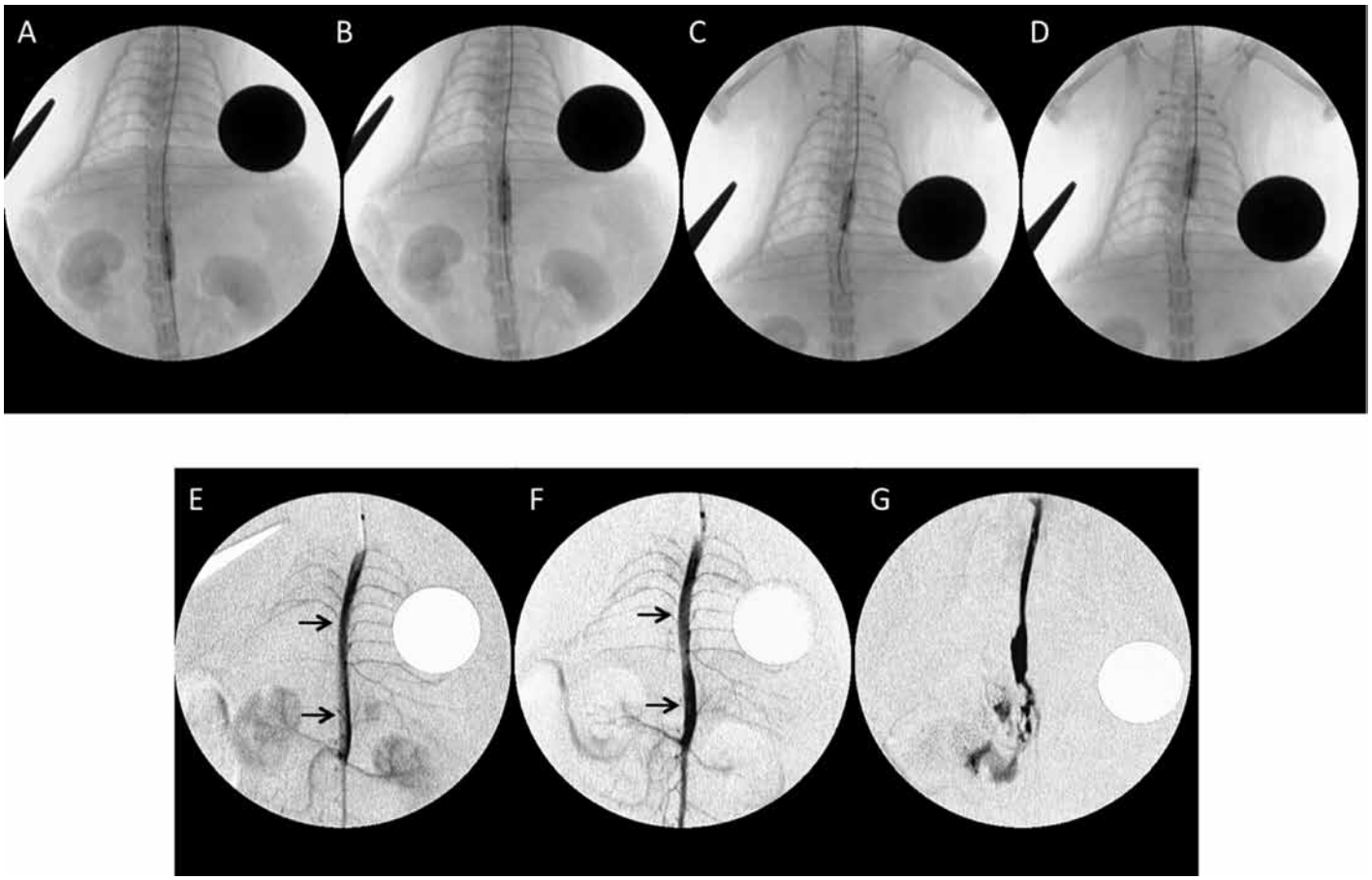

Figure 2. Anteroposterior radiographs demonstrating the balloon-injury technique. The balloon was (A) inflated above the renal bifurcation to a pressure of 2 atm (manual barometer) and then (B) pulled and rotated to just below the diaphragm, 4 successive times. (C) The thoracic aortic injury was done in similar fashion from above the diaphragm to (D) a few millimeters distal to the aortic arch. The radiopaque circle represents a 19-mm coin. Aortograms obtained (E) before and (F) after balloon injury demonstrate initial dilatation of the injured thoracic and abdominal aorta (arrows). (G) Occasionally, the induced injury would be complicated by aortic dissection and rupture (extravasation).

Statistical analysis. All results are reported as mean ± SEM. Statistical analysis was performed by using SigmaPlot software (version 11, Systat Software, Chicago, IL). Differences between the groups were assessed by 2-way ANOVA with post hoc testing (Student–Newman–Keuls test). The relationship between angiographic and histologic changes was assessed by Pearson correlation. A P value of less than 0.05 was considered to be statistically significant.

Results

At the time of follow-up, all rats appeared healthy. Mean body weight was significantly ($P < 0.05$) greater in OZR compared with LZR (10 wk: LZR, 343.3 g; OZR, 491.7 g; 12 wk: LZR, 374.2 g; OZR, 526.6 g; 14 wk: LZR, 398.9 g; OZR, 573.8; 20 wk: LZR, 431.1 g; OZR, 654.2 g). Five rats died perioperatively due abdominal (LZR, $n = 3$; OZR, $n = 1$) or thoracic (LZR $n = 1$) aortic injury including dissection, thrombosis, and rupture (Figure 1). Two rats (OZR, $n = 2$) developed paraplegia as a result of spinal cord ischemia and died 3 and 7 d after BI, respectively.

Lumen diameter. The baseline diameter of the thoracic aorta was 2.2 ± 0.1 mm in LZRs and 2.4 ± 0.1 mm in OZR (Table 1). The baseline diameter of the abdominal aorta was 2.3 ± 0.1 mm in LZR and 2.2 ± 0.0 mm in OZRs.

Relative to baseline measurements, the thoracic aorta of LZR had expanded 13.3% ± 9.3% at 4 wk after BI and 9.5% ± 4.3% at 10 wk. This continued expansion contrasted with an expansion (compared with baseline) of 1.0% ± 2.9% ($P = 0.016$) at 4 wk after BI in the thoracic aorta of OZR and a stenosis of 2.8% ± 1.6% ($P = 0.003$) at 10 wk. At 2 wk after BI, there were no significant differences in the thoracic aortograms of the OZR and LZR ($P = 0.585$).

Two weeks after BI, the abdominal aorta of OZR were expanded or unchanged (2.2% ± 2.8%), compared with an initial narrowing of 5.6% ± 1.8% ($P = 0.044$) in LZR. At 4 wk, the abdominal aorta of OZR had narrowed 6.9% ± 3.6%, compared with expansion of 0.4% ± 1.3% ($P = 0.036$) in LZR. Furthermore, 10 wk after BI, the abdominal aorta of OZR had narrowed 8.3% ± 1.1% compared with expansion of 2.4% ± 2.2% in LZR ($P < 0.001$; Figure 3).

Intimal hyperplasia. Visual examination by light microscopy revealed a highly irregular neointima formation in both the abdominal and thoracic aorta of OZR and LZR after BI (Figure 4). OZR had increased ($P < 0.01$) neointima formation in the abdominal and thoracic aortas of compared with LZR at 2, 4, and 10 wk after BI (Table 1 and Figure 5). This change was associated with a significant increase in the intimal:medial thickness ratio in the OZR aorta compared with LZR at 4 wk (thoracic: OZR, 0.39 ± 0.11;

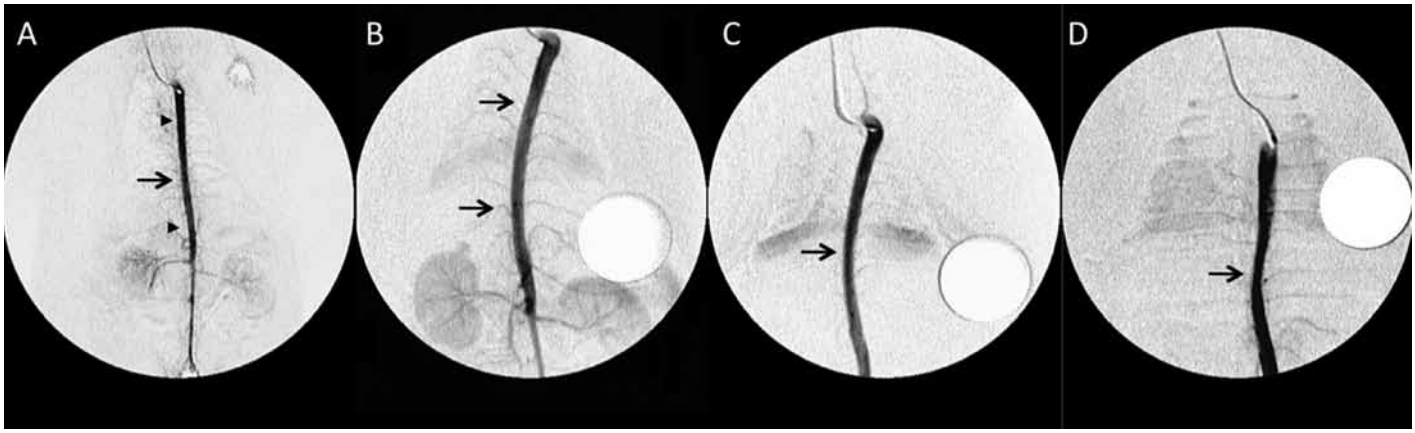

Figure 3. Anteroposterior aortograms before (baseline) and after balloon injury. (A) At baseline, there is a larger proximal thoracic aorta (upper arrowhead) that tapers down around the diaphragm (arrow) and becomes widens again at the renal artery bifurcation (lower arrowhead). (B) At 4 and 10 wk after balloon injury, the thoracic and abdominal aorta of LZ rats expanded when compared with the diameters at baseline (arrows; magnification, 2×). (C and D) The abdominal aortas of OZ rats became stenotic (arrows; magnification, magnification, 2×) when compared with baseline values.

Table 1. Angiographic and histomorphometric analysis of descending aortas from lean (LZ) and obese (OZ) Zucker rats at various times after balloon injury

			Baseline diameter (mm)	Postinjury diameter (mm)	Expansion (%)[a]	Medial thickness (μm)	Peak intimal thickness (μm)	intimal:medial thickness ratio
Thoracic aorta								
	2 wk							
		LZ (n = 4)	2.32 ± 0.10	2.64 ± 0.03	1.76 ± 1.97	85.9 ± 2.0	7.6 ± 4.6	0.09 ± 0.05
		OZ (n = 4	2.61 ± 0.04	3.00 ± 0.06	4.73 ± 1.03	105.4 ± 2.0	29.0 ± 6.5	0.27 ± 0.05
	4 wk							
		LZ (n = 5)	2.35 ± 0.03	2.69 ± 0.09	13.30 ± 9.29	91.1 ± 0.2	3.3 ± 3.3	0.04 ± 0.04
		OZ (n = 5)	2.29 ± 0.14	2.78 ± 0.12	1.02 ± 2.91	113.6 ± 5.4	45.1 ± 14.3	0.39 ± 0.11
	10 wk							
		LZ (n = 8)	2.07 ± 0.07	2.77 ± 0.08	9.47 ± 4.27	103.2 ± 2.8	10.4 ± 5.2	0.10 ± 0.05
		OZ (n = 9)	2.33 ± 0.08	2.83 ± 0.06	–2.78 ± 1.65	99.0 ± 4.0	38.6 ± 6.1	0.39 ± 0.05
Abdominal aorta								
	2 wk							
		LZ (n = 4)	2.38 ± 0.06	2.51 ± 0.08	–5.59 ± 1.78	98.5 ± 9.5	12.3 ± 4.1	0.13 ± 0.05
		OZ (n = 4	2.32 ± 0.01	2.63 ± 0.17	2.22 ± 2.77	104.8 ± 10.9	33.2 ± 4.8	0.31 ± 0.01
	4wk							
		LZ (n = 5)	2.40 ± 0.07	2.41 ± 0.07	0.40 ± 1.33	102.5 ± 5.9	17.7 ± 5.4	0.17 ± 0.05
		OZ (n = 5)	2.09 ± 0.04	2.32 ± 0.03	–6.88 ± 3.64	109.6 ± 6.5	61.3 ± 12.0	0.54 ± 0.07
	10 wk							
		LZ (n = 8)	2.03 ± 0.04	2.53 ± 0.07	2.36 ± 2.24	103.2 ± 2.8	27.0 ± 11.6	0.26 ± 0.11
		OZ (n = 9)	2.25 ± 0.05	2.56 ± 0.08	–8.34 ± 1.10	117.5 ± 8.4	83.0 ± 11.5	0.70 ± 0.07

Data are mean ± SEM. Differences between LZ and OZ groups were determined by groupwise ANOVA.
[a]A negative value indicates stenosis at the indicated percentage.

LZR, 0.04 ± 0.04; P = 0.001; abdominal: OZR, 0.54 ± 0.07; LZR, 0.17 ± 0.05; P = 0.008), and 10 wk (thoracic: OZR, 0.39 ± 0.05; LZR, 0.10 ± 0.05; P < 0.001; abdominal: OZR, 0.70 ± 0.07; LZR, 0.26 ± 0.11; P < 0.001).

No correlation was found between the degree of angiographic stenosis in the injured OZR thoracic and abdominal aorta, the amount of neointimal formation (as measured by the I:M thickness ratio), or the peak intimal or medial thickness.

Discussion

Experimental models in various animal species have been used to study the pathologic intimal formation as a response of vessel wall damage. The rat carotid artery BI model is one of the most convenient, rapid, and thoroughly investigated models for the assessment and treatment of intimal hyperplasia.[11,17] However, the carotid artery is too small to test the presently available endovascular devices used in the clinical setting. Furthermore, in contrast to human arteries, the rat carotid artery contains a much thinner

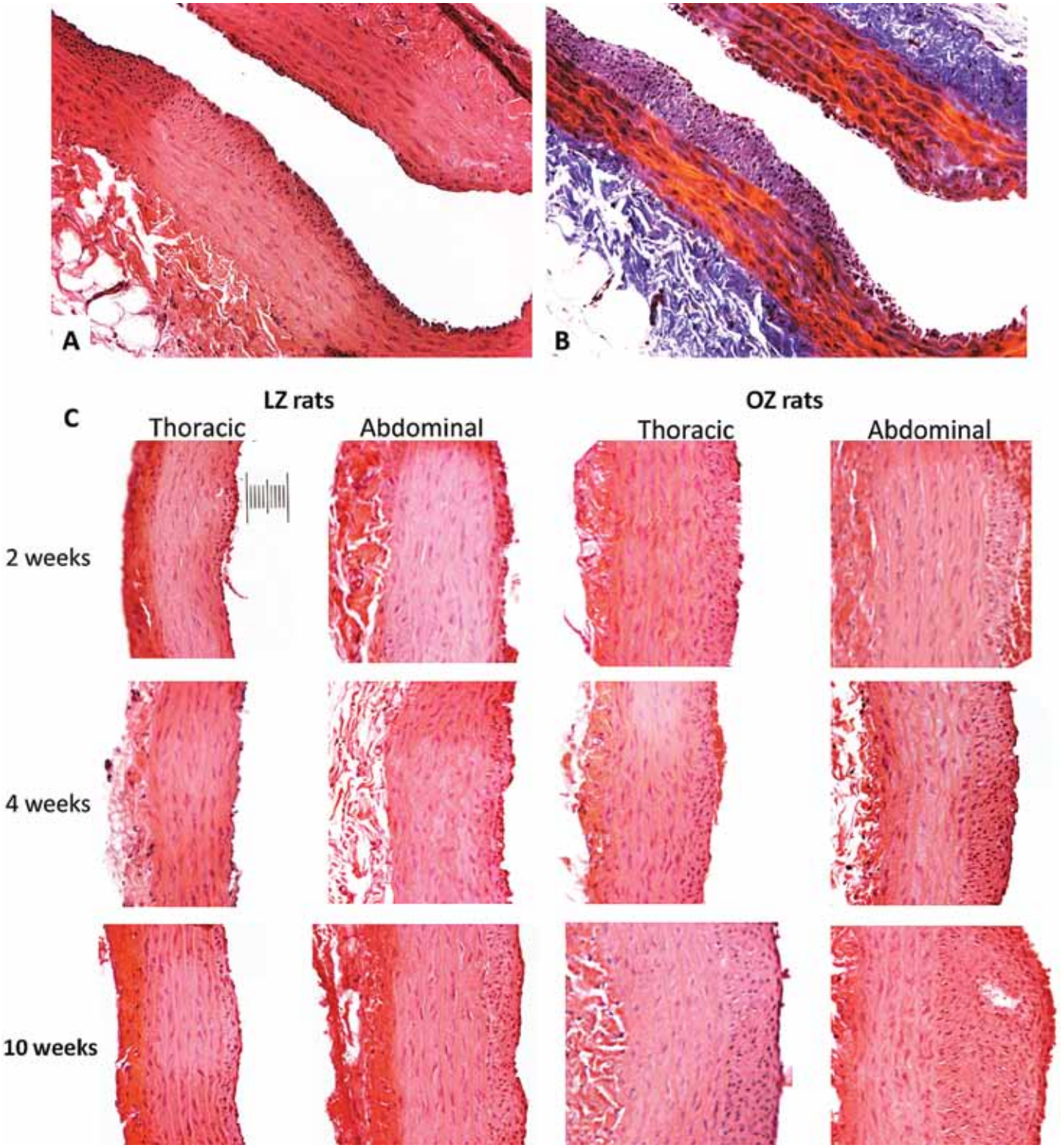

Figure 4. Staining with (A) hematoxylin and eosin and (B) trichrome of cross-sections of descending aorta after balloon injury revealed highly irregular neointima formation in the abdominal and thoracic aorta of OZ and LZ rats. Original magnification, 100×. (C) Staining with hematoxylin and eosin of cross-sections of the thoracic and abdominal aortas in LZ and OZ rats at 2, 4, and 10 wk after balloon injury show temporal increases in neointimal formation in the abdominal and thoracic aortas of OZ compared with LZ rats. Original magnification, 40×.

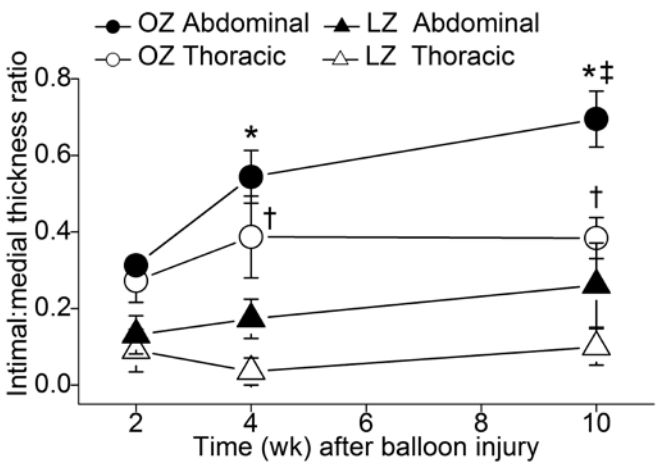

Figure 5. Intimal:medial thickness ratios (mean ± SEM [bar]) of the thoracic and abdominal aortas of OZ and LZ rats (2 wk: $n = 4$ for both LZ and OZ rats; 4 wk, $n = 5$ for both LZ and OZ rats; 10 wk: LZ, $n = 8$; OZ, $n = 9$) plotted against time (wk). *, The ratio for the abdominal aorta was significantly greater in OZ rats than LZ rats at 4 wk ($P = 0.008$) and 10 wk ($P < 0.001$) after balloon injury. †, The ratio for the thoracic aorta was greater in OZ rats than LZ rats at 4 wk ($P = 0.001$) and 10 wk ($P < 0.001$) after balloon injury. ‡, The ratio in the abdominal aorta of OZ rats was significantly ($P = 0.012$) greater at 10 wk compared with 2 wk after balloon injury.

subintimal layer and lower elastin and higher collagen contents in the tunica media.[22] In the current study, the rat abdominal and thoracic aorta, which are wider than the carotid artery, were validated as an alternative model to be used for the evaluation of arterial response after endovascular techniques. Currently available endovascular catheters, wires, balloons, and stents, provide enhanced access and flexibility. This property allows their use in this small animal model. In humans, the composite coronary artery diameter ranges from 1.9 to 5.4 mm (average, 3.4 ± 0.5 mm), and the average diameter of the middle cerebral artery is 3 to 5 mm.[1,10] These measurements correspond to the baseline diameter of the descending aortas in of LZR and OZR. The rat thoracic and abdominal aortas are large enough to deploy and potentially test most currently available coronary and intracranial stents with their delivery systems.

In our study, the thoracic aorta of LZR exhibited the least amount of intimal hyperplasia, where 9 of 17 displayed no intimal hyperplasia at multiple time points. Concurrently, the thoracic aorta of these rats developed the largest amount of adaptive remodeling at 4 and 10 wk after BI, as measured by the percentage of expansion. Although the abdominal aorta of LZR exhibited more intimal hyperplasia than did their thoracic aorta, it was still significantly less than that in the abdominal aortas of OZR. Abdominal aortas in LZR showed a trend toward adaptive remodeling 4 and 10 wk after BI. This finding is in agreement with prior reports demonstrating that the abdominal aorta of Wistar rats compensates to intimal hyperplasia by adaptive remodeling.[5] The abdominal aorta of OZR responded differently and developed the largest amount of intimal hyperplasia and constrictive remodeling in our study. Both of these responses increased with time and were significantly different than those of their lean counterparts. The thoracic aorta in OZR expanded initially but showed a trend to constriction at 10 wk after BI. In addition, the thoracic aorta in OZR exhibited a significantly more intimal hyperplasia than did LZR. Previous reports have documented a similar propensity in the carotid artery of OZR to develop intimal hyperplasia after BI.[18,21] Our results not only demonstrate increased neointima formation in the aorta of OZR but also a propensity toward constrictive remodeling.

We did not find a correlation between the degree of angiographic stenosis or expansion and the amount of neointimal formation at any time point. This result suggests, as previously reported,[14] that vessel wall remodeling and neointima formation are 2 separate processes. Multiple factors may account for the different intimal hyperplasia and arterial remodeling responses observed in the thoracic and abdominal aortas of LZR and OZR after BI, including an artery-type-dependent variation of both synthetic and contractile smooth muscle cells, the number of vasa vasorum in the tunica adventitia, and the increasingly important role of the tunica adventitia in inflammation, growth, and repair.[7,10,14]

The abdominal aortas of both LZR and OZR developed intimal hyperplasia that continued to increase until at least 10 wk after injury and perhaps beyond. Compared with their abdominal aortas, the thoracic aortas of both rat groups had less intimal hyperplasia that tended to increase with time. This trait has been demonstrated before and is different from that in the rat carotid injury model, in which intimal hyperplasia peaks between 14 to 28 d after BI.[2,5,13] We observed irregular or patchy intimal hyperplasia in the descending aorta of Zucker rats, and this pattern is different from the uniformly circumferential response observed in the carotid BI model and the abdominal aorta–common iliac artery models reported elsewhere.[5,15,17] In addition, another previous study had reported a similar, less uniform and less rapid, response in a rat model of aortic BI.[13] We hypothesize that our results reflect a smaller vessel lumen-to-balloon ratio (0.6 to 0.8), the use of a semicompliant balloon, and the plane of attachment of the descending aorta and its segmental branches, for which the anterior aspect is free but the posterior sides are fixed.

In conclusion, the model we use here provides less invasive access to the rat's descending aorta and is compatible with many endovascular instruments used in clinical practice. The rat aorta is large enough to potentially deploy and test coronary and intracranial stents. Neointimal formation after BI is enhanced in the abdominal and thoracic aortas of OZR. BI tends to induce constrictive remodeling in the OZR aorta as compared with the adaptive remodeling seen in the LZR aorta.

Acknowledgments

We thank Dr Gene Bidwell for providing statistical consultation, Dr Lynne Orozco for reviewing the manuscript, Dr Juan Carlos Pisarello for the illustration, and Ms Bevelyn Perkins for slide preparation. This work was supported by the Departments of Anatomy, Neurosurgery, and Radiology at the University of Mississippi Medical Center (Jackson, MS).

References

1. **Aronson D, Bloomgarden Z, Rayfield EJ.** 1996. Potential mechanisms promoting restenosis in diabetic patients. J Am Coll Cardiol **27:**528–535.
2. **Clowes AW, Reidy MA, Clowes MM.** 1983. Mechanisms of stenosis after arterial injury. Lab Invest **49:**208–215.
3. **Ferguson GG, Eliasziw M, Barr HW, Clagett GP, Barnes RW, Wallace MC, Taylor DW, Haynes RB, Finan JW, Hachinski VC, Barnett HJ.** 1999. The North American symptomatic carotid endarterectomy trial: surgical results in 1415 patients. Stroke **30:**1751–1758.

4. **Forte A, Esposito S, De Feo M, Galderisi U, Quarto C, Esposito F, Renzulli A, Berrino L, Cipollaro M, Agozzino L, Cotrufo M, Rossi F, Cascino A.** 2003. Stenosis progression after surgical injury in Milan hypertensive rat carotid arteries. Cardiovasc Res **60:**654–663.
5. **Gabeler EE, van Hillegersberg R, Statius van Eps RG, Sluiter W, Gussenhoven EJ, Mulder P, van Urk H.** 2002. A comparison of balloon injury models of endovascular lesions in rat arteries. BMC Cardiovasc Disord **2:**16.
6. **Glagov S.** 1994. Intimal hyperplasia, vascular modeling, and the restenosis problem. Circulation **89:**2888–2891.
7. **Goldberg ID, Stemerman MB, Ransil BJ, Fuhro RL.** 1980. In vivo aortic muscle cell growth kinetics. Differences between thoracic and abdominal segments after intimal injury in the rabbit. Circ Res **47:**182–189.
8. **Hammoud T, Tanguay JF, Bourassa MG.** 2000. Management of coronary artery disease: therapeutic options in patients with diabetes. J Am Coll Cardiol **36:**355–365.
9. **Institute for Laboratory Animal Research.** 1996. Guide for the care and use of laboratory animals. Washington (DC): National Academies Press.
10. **Jain KK.** 1964. Some observations on the anatomy of the middle cerebral artery. Can J Surg **7:**134–139.
11. **Johnson GJ, Griggs TR, Badimon L.** 1999. The utility of animal models in the preclinical study of interventions to prevent human coronary artery restenosis: analysis and recommendations. On behalf of the Subcommittee on Animal, Cellular, and Molecular Models of Thrombosis and Haemostasis of the Scientific and Standardization Committee of the International Society on Thrombosis and Haemostasis. Thromb Haemost **81:**835–843.
12. **Kissin I, Morgan PL, Smith LR.** 1983. Comparison of isoflurane and halothane safety margins in rats. Anesthesiology **58:**556–561.
13. **Koletsky S, Snajdar RM.** 1981. Atherosclerosis following balloon catheter injury to the carotid artery and the aorta of hypertensive rats with normolipidemia or hyperlipidemia. Am J Pathol **103:**105–115.
14. **Kundi R, Hollenbeck ST, Yamanouchi D, Herman BC, Edlin R, Ryer EJ, Wang C, Tsai S, Liu B, Kent KC.** 2009. Arterial gene transfer of the TGFβ signalling protein Smad3 induces adaptive remodelling following angioplasty: a role for CTGF. Cardiovasc Res **84:**326–335.
15. **Langeveld B, Roks AJ, Tio RA, van Boven AJ, van der Want JJ, Henning RH, van Beusekom HM, van der Giessen WJ, Zijlstra F, van Gilst WH.** 2004. Rat abdominal aorta stenting: a new and reliable small animal model for in-stent restenosis. J Vasc Res **41:**377–386.
16. **Mathé D.** 1995. Dyslipidemia and diabetes: animal models. Diabete Metab **21:**106–111.
17. **Orozco LD, Liu H, Chen BB, Fratkin JD, Perkins E.** 2011. Angiographic evaluation of the rat carotid balloon injury model. Exp Mol Pathol **91:**590–595.
18. **Park SH, Marso SP, Zhou Z, Foroudi F, Topol EJ, Lincoff AM.** 2001. Neointimal hyperplasia after arterial injury is increased in a rat model of non-insulin-dependent diabetes mellitus. Circulation **104:**815–819.
19. **Pasterkamp G, de Kleijn DP, Borst C.** 2000. Arterial remodeling in atherosclerosis, restenosis and after alteration of blood flow: potential mechanisms and clinical implications. Cardiovasc Res **45:**843–852.
20. **Paulson DJ, Tahiliani AG.** 1992. Cardiovascular abnormalities associated with human and rodent obesity. Life Sci **51:**1557–1569.
21. **Shelton J, Wang D, Gupta H, Wyss JM, Oparil S, White CR.** 2003. The neointimal response to endovascular injury is increased in obese Zucker rats. Diabetes Obes Metab **5:**415–423.
22. **Sims FH.** 1989. A comparison of structural features of the walls of coronary arteries from 10 different species. Pathology **21:**115–124.
23. **Stamler J, Vaccaro O, Neaton JD, Wentworth D.** 1993. Diabetes, other risk factors, and 12-y cardiovascular mortality for men screened in the Multiple Risk Factor Intervention Trial. Diabetes Care **16:**434–444.
24. **Standley PR, Rose KA, Sowers JR.** 1995. Increased basal arterial smooth muscle glucose transport in the Zucker rat. Am J Hypertens **8:**48–52.
25. **Winocour PD, Richardson M, Kinlough-Rathbone RL.** 1993. Continued platelet interaction with de-endothelialized aortae associated with slower re-endothelialization and more extensive intimal hyperplasia in spontaneously diabetic BB Wistar rats. Int J Exp Pathol **74:**603–613.